Heliyon 6 (2020) e03922

Contents lists available at ScienceDirect

Heliyon

journal homepage: www.cell.com/heliyon

Research article

# Grb7-derived calmodulin-binding peptides inhibit proliferation, migration and invasiveness of tumor cells while they enhance attachment to the substrate

Juan Alcalde [a,b,1], María González-Muñoz [b,1], Antonio Villalobo [b,c,*]

[a] Department of Biochemistry and Molecular Biology, Faculty of Medicine, Complutense University, Madrid, Spain
[b] Department of Cancer Biology, Instituto de Investigaciones Biomédicas, Consejo Superior de Investigaciones Científicas and Universidad Autónoma de Madrid, Arturo Duperier 4, E-28029 Madrid, Spain
[c] Cancer and Human Molecular Genetics Area – Oto-Neurosurgery Research Group, University Hospital La Paz Research Institute (IdiPAZ), Paseo de la Castellana 261, E-28046, Madrid, Spain

ARTICLE INFO

*Keywords:*
Biochemistry
Cell biology
Molecular biology
Cancer research
Calmodulin
Cell-penetrating peptides
Epidermal growth factor receptor
Grb7
Tumor cells

ABSTRACT

The growth factor receptor bound protein 7 (Grb7) is a $Ca^{2+}$-dependent calmodulin (CaM)-binding adaptor protein implicated, among other functions, in cell proliferation, migration and tumor-associated angiogenesis. The goal of this study was to determine whether a peptide based on the CaM binding site of Grb7 disrupts cellular processes, relevant for the malignancy of tumor cells, in which this adaptor protein is implicated. We designed synthetic myristoylated and non-myristoylated peptides corresponding to the CaM-binding domain of human Grb7 with the sequence $^{243}$RKLWKRFFCFLRRS$^{256}$ and a variant peptide with the mutated sequence RKLERFFCFLRRE (W246E-ΔK247-S256E). The two non-myristoylated peptides bind dansyl-CaM with higher efficiency in the presence than in the absence of $Ca^{2+}$ and they enter into the cell, as tested with 5(6)-carboxytetramethylrhodamine (TAMRA)-labeled peptides. The myristoylated and non-myristoylated peptides inhibit the proliferation, migration and invasiveness of A431 tumor cells while they enhance their adhesion to the substrate. The myristoylated peptides have stronger inhibitory effect than the non-myristoylated counterparts, in agreement with their expected higher cell-permeant capacity. The myristoylated and non-myristoylated W246E-ΔK247-S256E mutant peptide has a lesser inhibitory effect on cell proliferation as compared to the wild-type peptide. We also demonstrated that the myristoylated peptides were more efficient than the CaM antagonist *N*-(6-aminohexyl)-5-chloro-1-naphthalenesulfonamide (W-7) inhibiting cell migration and equally efficient inhibiting cell proliferation.

## 1. Introduction

The growth factor receptor bound protein 7 (Grb7) is a modular Src homology domain 2 (SH2)-containing adaptor protein that signals upon interaction with phospho-Tyr residues in different active tyrosine-kinase receptors and other phospho-proteins. Grb7 is phosphorylated by focal adhesion kinase (FAK) and is implicated, among other functions, in cell proliferation and cell migration [1, 2, 3, 4]. In some tumor cells, such as breast, ovarian, cervical and esophagus carcinomas, among others, Grb7 is overexpressed with the erythroblastic leukemia viral oncogene homologue 2 receptor (ErbB2) enhancing invasiveness and their proliferative capacity [5, 6, 7, 8, 9]. This is facilitated by the location of both genes in an amplicon at the chromosome locus 17q12-21 amplified in some tumors [10]. The epidermal growth factor receptor (EGFR) is also implicated in the malignancy of ErbB2/Grb7 overexpressing tumor cells [11]. In this context, the recruitment of Grb7 by ligand-activated EGFR induces activation of Ras and the mitogen activated protein kinase (MAPK) pathway resulting in cell proliferation [12, 13]. Similarly, integrins engagement to fibronectin induces FAK-mediated Grb7 phosphorylation and activation of the GTPase Rac1 leading to cell migration [13]. Using different experimental systems, it was shown that Grb7 also participates in tumor-associated angiogenesis [14, 15]. Grb7 also plays a prominent role in the invasiveness of the highly malignant triple-negative breast tumors (lacking ErbB2, estrogen and progesterone

* Corresponding author.
*E-mail address:* antonio.villalobo@idipaz.es (A. Villalobo).
[1] These authors equally contributed to this work.

https://doi.org/10.1016/j.heliyon.2020.e03922
Received 30 August 2019; Received in revised form 5 February 2020; Accepted 30 April 2020

receptors) [16, 17]. A variant Grb7 denoted Grb7V, lacking the SH2 domain, is also expressed in some tumor cells contributing to its malignancy [6, 18].

Grb7, as well as the Grb7-family members Grb10 and Grb14, are $Ca^{2+}$-dependent calmodulin (CaM)-binding proteins [15, 19]. In human Grb7 the CaM-binding domain (CaM-BD) with the sequence $^{243}$RKLWKRFFCFLRRS$^{256}$ is located in the proximal region of the pleckstrin homology (PH) domain [15, 19] and overlaps the nuclear-localization sequence [20]. CaM binding to the CaM-BD of Grb7 has important functional roles. Thus, it has been shown that a deletion mutant lacking the CaM-BD (Grb7Δ) prevents its translocation to the nucleus, while CaM inhibition by *N*-(6-aminohexyl)-5-chloro-1-naphthalenesulfonamide (W-7) enhances its nuclear localization [20]. This may be relevant for the known association of Grb7 to the transcriptional regulator FHL2 [21]. Moreover, normal and tumor cells transfected with Grb7Δ present impaired capacity of attachment to the extracellular matrix and to migrate [14, 22], inhibiting as well cell proliferation, tumor-associated angiogenesis and the growth of tumors derived from implanted glioma transfected cells *in vivo* [14].

Several hundred CaM-binding proteins have been shown to participate in signaling pathways regulating multiple cellular functions, including cell proliferation and cell motility. These processes are dysregulated in tumor cells, contributing in this manner to the progression, invasiveness and metastatic capacity of malignant neoplasia [23, 24]. Grb7 has been considered a potential target for anti-tumor therapy [25, 26]. Given its functional importance, the SH2 domain present in many proteins, including Grb7, has been explored as target for therapeutic intervention [27]. In the case of Grb7, a series of cell-penetrating peptides that interact and block its SH2 domain have been shown to inhibit Grb7-driven cellular functions in tumor cells [28, 29, 30, 31]. Moreover, the anti-tumor activity of cell-penetrating peptides, myristoylated [32] or tagged with a hydrophobic sequence [26] to allow cell entry, targeting other proteins, has been demonstrated. The aim of this study was to explore whether a peptide based on the CaM-BD of Grb7 could disrupt relevant tumor cell functions in which this adaptor protein is implicated.

In this report, we show the effect of a myristoylated and non-myristoylated cell-penetrating peptide with a sequence corresponding to the CaM-BD of human Grb7, and a mutated variant, on the proliferation, adhesion, migration and invasiveness of A431 tumor cells. These peptides are expected to sequester intracellular CaM affecting multiple CaM-dependent systems implicated in signaling pathways involved in these cellular functions [23, 24], and/or more specifically to act as decoys preventing the binding of CaM to Grb7. We selected A431 cells as an experimental model based on the fact that this human tumor cell line overexpresses the EGFR [33] which is regulated by CaM [34]; and also expresses the adaptor protein Grb7, which is regulated by both the EGFR [35] and CaM [14, 15, 20, 22]. In addition, the EGFR and Grb7 both are implicated in cell proliferation and migration processes [1, 2, 3, 4].

## 2. Results

### 2.1. Characterization of peptides derived from the CaM-BD of Grb7

Two synthetic peptides were custom-designed as follow: i) a wild-type peptide with the sequence $^{243}$RKLWKRFFCFLRRS$^{256}$ corresponding to the CaM-BD of human Grb7 [15,19]; and ii) a mutated peptide lacking K247 plus two point-mutations (W246E and S256E) with the sequence RKLERFFCFLRRE (W/E-ΔK-S/E). Suppl. Figure S1 shows the helical wheel projection of the wild-type peptide which has all basic residues located in one-half side of the helix, while the non-polar residues are located in the opposite side. This is characteristic of many CaM-binding sequences [36]. The most significant feature of the W/E-ΔK-S/E mutant peptide is the location of the two acidic residues in opposite sides of the helix, which has one half enriched in basic residues and the other enriched in non-polar residues. These peptides were tested for their capacity to bind CaM in the absence and presence of $Ca^{2+}$ using dansyl-CaM by monitoring fluorescence emission. Suppl. Figure S2 shows that wild-type and W/E-ΔK-S/E mutant peptides bind CaM in the presence of $Ca^{2+}$, and to a lesser extent in its absence (presence of EGTA). When the concentration of the wild-type peptide was increased up to 12 μg/ml the binding of dansyl-CaM in the presence of $Ca^{2+}$ was ~40% higher than in its absence (presence of EGTA). In contrast, the binding of the W/E-ΔK-S/E mutant peptide to dansyl-CaM in the presence of $Ca^{2+}$ was 2.5-fold higher than in its absence (presence of EGTA). We previously demonstrated the $Ca^{2+}$-dependent CaM-binding capacity of the Grb7-derived wild-type peptide, together with two other peptides corresponding to the CaM-BDs of the Grb7-family members Grb10 and Grb14, using 5(6)-carboxytetramethylrhodamine (TAMRA)-labeled peptides measuring fluorescence polarization [19]. In this work, it was shown that occupancy of a single EF-hand $Ca^{2+}$-binding site, of the four containing CaM, allows efficient binding to the Grb7-derived peptide [19].

We postulated that the wild-type peptide corresponding to the CaM-binding domain of Grb7 could sequester endogenous CaM inhibiting CaM-dependent systems in living cells. The peptide was synthesized with and without a myristoyl group in its N-terminus to favor its entry in the cell. To ascertain the inhibitory capacity of the wild-type Grb7-derived peptide in a CaM-binding protein, we tested the action of both versions of this peptide on the ligand-dependent activation of the EGFR. A431 cells overexpress the EGFR [33] and also express Grb7 [37]. Therefore, these cells were considered a good experimental system for testing the Grb7-derived wild-type peptide on EGFR activation. This receptor binds CaM and phospho-Tyr-CaM in a $Ca^{2+}$-dependent manner positively regulating its activity [38, 39, 40, 41, 42]. We observe in Figure 1 that both versions of the Grb7-derived peptide inhibit the ligand-dependent activation of the EGFR, and the inhibition exerted by the myristoylated peptide was stronger than the non-myristoylated one as expected. This agrees with the inhibitory action that a myristoylated peptide corresponding to the CaM-BD of myosin light-chain kinase (MLCK), and a variant peptide corresponding to the CaM-BD of the EGFR tagged with an hydrophobic cell-penetrating TAT sequence, exert on the ligand-dependent activation of both the EGFR and ErbB2, a tyrosine kinase receptor of the same family that the EGFR [26, 41].

As the non-myristoylated wild-type peptide has a strong inhibitory action on the ligand-dependent activation of the EGFR, it was suspected to be able to penetrate into the cells, similarly to the penetration of its myristoylated counterpart, as the cell-penetrating capacity of myristoylated peptides is well documented [43]. We tagged the wild-type and W/E-ΔK-S/E mutant peptides with the fluorescent probe TAMRA, and tested the capacity of these peptides to be internalized. As shown in Suppl. Figure S3, the cell fluorescence signal measured by cell cytometry was positive with the two TAMRA-labeled peptides, while no significant signal was detected using free TAMRA. To determine the intracellular location of the internalized peptides, we observed living cells treated with the TAMRA-peptides. Figure 2 shows that the signal of the TAMRA-peptides was located at the plasma membrane and in intracellular vesicles.

Due to the internalization of the non-myristoylated peptides, it was expected that they were able to sequester intracellular CaM as well, as may occur with the myristoylated ones. Therefore, we proceeded to test their effects on the proliferation, migration and adhesion of living tumor cells, as CaM is known to participate in signaling pathways controlling these processes [23, 24].

### 2.2. Effect of W-7/W-12 and Grb7-derived peptides on cell proliferation and anchorage-independent growth

Before testing the effect of peptides derived from the CaM-BD of Grb7, we tested the effect of known CaM antagonists on the proliferation and anchorage-independent growth of A431 cells. Figure 3A shows that the epidermal growth factor (EGF) strongly inhibits the proliferation of this

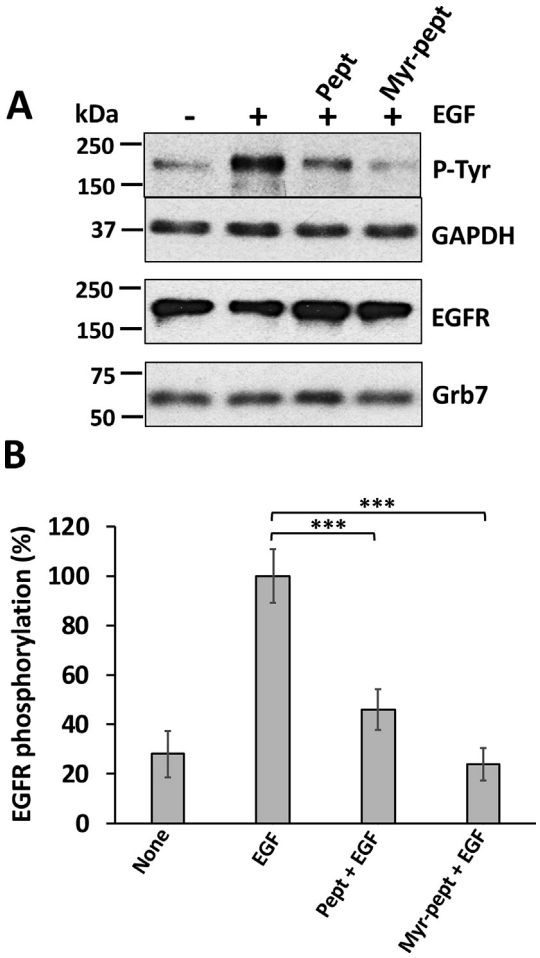


**Figure 1.** The wild-type peptide inhibits ligand-dependent activation of the EGFR. Cells grown to confluency were serum-starved overnight and incubated as indicated in the absence and presence of 50 μg/ml of the non-myristoylated wild-type peptide (*Pept*) and its myristoylated form (*Myr-pept*) during 15 min at room temperature. The control in the absence of peptides contains 1% (v/v) DMSO (vehicle). Thereafter, cells were incubated in the absence (-) and presence (+) of 10 nM EGF for 5 min, the reaction arrested with ice-cold 10% (w/v) trichloroacetic acid and processed by SDS-PAGE and Western blot using anti-phospho-Tyr, anti-EGFR, anti-Grb7 and anti-GAPDH antibodies as described in the Experimental section. Representative blots (*A*) and a plot (*B*) with the mean ± SEM (n = 6) densitometric quantification of the phospho-Tyr band, corresponding to phosphorylated-EGFR corrected by the corresponding loading control (GAPDH, Grb7 or total EGFR) of six independent experiments are presented. Statistically significant differences were calculated using the Student's *t*-test (***$p < 0.001$). The Western blots were developed from segments of the PVDF membranes of adequate size, and the images were cropped from the original films at different exposure times, processed for optimal brightness and contrast, and compressed or stretched to attain segments of the same size to prepare the figure. (original uncropped Western blots are shown in Supplementary Material).

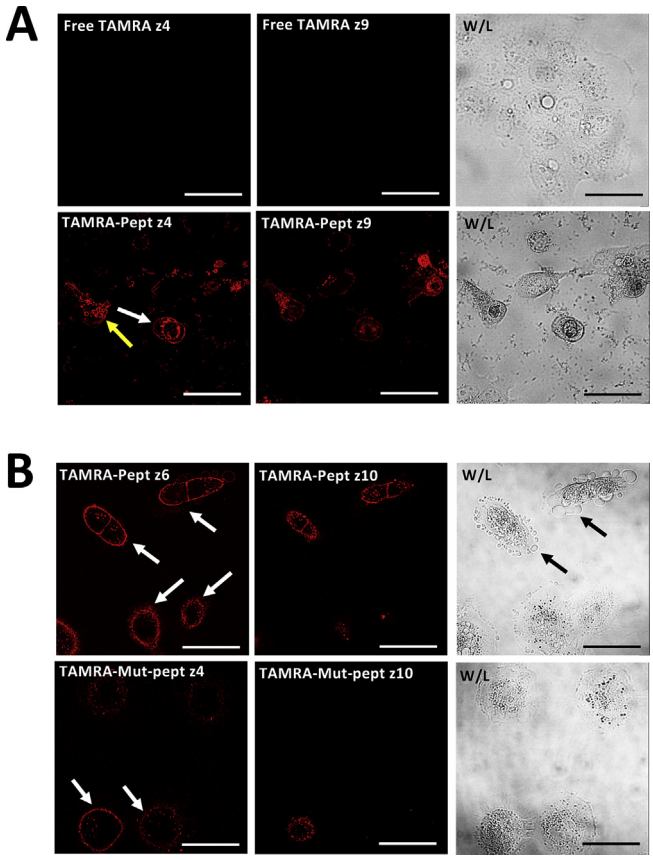


**Figure 2.** Internalization of the peptides. Microphotographs of living cells treated overnight (*A*) or during 5 min (*B*) with the TAMRA-labeled wild-type and W/E-ΔK-S/E mutant peptides, and gently washed thereafter, were taken by confocal microscopy as described in the Experimental section. TAMRA fluorescence (*Red*) and white light images (*W/L*) are shown. The white and yellow arrows point to segments of the plasma membrane and membranes of intracellular vesicles, respectively, where the TAMRA-labeled peptides signal was located. The black arrows point to membrane blebbing in cells treated with the wild-type TAMRA-labeled peptide. The bars indicate 50 μm.

cell line in agreement with previous results [44, 45]. Similar inhibitory action of EGF was observed when anchorage-independent growth in soft agar was tested, particularly decreasing the size of the colonies (Figure 3B,C). W-7, a high-affinity CaM antagonist [46, 47, 48, 49], strongly inhibits cell proliferation in the absence and presence of EGF (Figure 3A) and the size and number of the colonies grown in soft agar in the presence of fetal bovine serum (FBS) (Figure 3B,C). In contrast, the low-affinity CaM antagonist analogue *N*-(4-amino-butyl)-2-naphthalenesulfonamide (W-12) [48,49] has very low effect on cell proliferation, as well as on the size and number of colonies formed in soft agar (Figure 3A-C).

As the effects of W-7/W-12 on cell proliferation are in agreement with previous results obtained in other cell lines [50, 51], we next tested the effect of the wild-type peptide $^{243}$RKLWKRFFCFLRRS$^{256}$ corresponding to the CaM-BD of human Grb7 [15], both with or without a myristoyl group attached to its N-terminus to facilitate its entry in the cell. We observed that the non-myristoylated (Figure 4A) and myristoylated (Figure 4B) wild-type peptides strongly inhibit the proliferation of the cells, both in the absence and presence of EGF, while the W/E-ΔK-S/E mutant peptide has a very small inhibitory effect in its non-myristoylated version (Figure 4A), but a rather significant inhibitory action in its myristoylated version (Figure 4B). Due to the difficulty of the peptides to diffuse through soft agar, we did not test the effect of the different peptides on anchorage-independent growth.

### 2.3. Effect of W-7/W-12 and Grb7-derived peptides on cell migration

We next studied the effect of the CaM antagonists W-7 and W-12 on the migration of A431 cells using the artificial wound healing assay. Figure 5A shows that in the absence of EGF the migration occurs without any delay and that the CaM antagonists increased the initial migration rate of the cells, particularly with the high affinity inhibitor W-7. In contrast, in the presence of EGF, the cells start to migrate after a few hours of inactivity in which retraction of the cell layer occurs slightly enhancing the width of the wound open area. In the presence of W-7 there is a significant slowdown of the maximum lineal migration rate

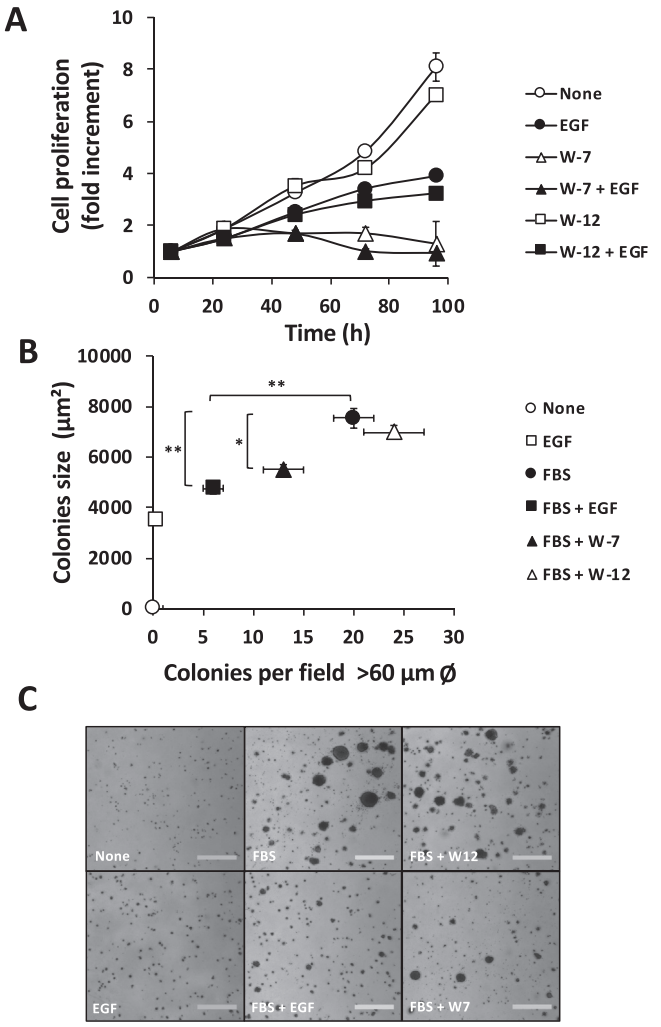


**Figure 3.** Effect of W-7/W-12 on cell proliferation and anchorage-independent growth. (*A*) Cells ($10^5$) were seeded in the presence of 0.5 % (v/v) FBS, and 10 nM EGF where indicated. Twenty-four hours thereafter, 15 μM W-7 or 15 μM W-12 was added where indicated. The control in the absence of inhibitors (*None*) was treated with 0.3% (v/v) DMSO (vehicle). Cell proliferation was measured by Crystal Violet staining as described in the Experimental section. The plot represents the mean ± SEM (n = 3) fold increment proliferation at the indicated times. Error bars are shown if larger than the symbols. (*B*) Cells ($10^5$) were seeded in soft-agar in the absence and presence of 10% (v/v) FBS, 10 nM EGF, 20 μM W-7 or 25 μM W-12 as indicated. Fresh medium with the indicated reagents was added every 3–4 days. Colonies were quantified using an Observer.Z1 microscope with a Cascade 1K camera and a 4x objective as indicated in the Experimental section 14 days after seeding. The plot represents the mean ± SEM (n = 4) number and size of the colonies >60 μm of diameter per microscopic field. Statistical significance differences (*$p < 0.05$, **$p < 0.01$) was determined using the Student's *t*-test. Error bars are shown if larger than the symbols. (*C*) Representative photographs of colonies in the absence and presence of 10% (v/v) FBS, 10 nM EGF, 20 μM W-7 or 25 μM W-12 as indicated. The scale bar indicates 500 μm.

occurring approximately at 25–35 h in the presence of EGF, while this is not observed with the low affinity inhibitor W-12. Figure 5B shows the width of the wounds at 0 and 30 h in the different assay conditions tested.

We tested the effect of the non-myristoylated and myristoylated peptides in the absence and presence of EGF on cell migration using the same technique. Figure 6A and Suppl. Figure S4 show that the non-myristoylated wild-type peptide strongly inhibits EGF-dependent and EGF-independent cell migration, while the W/E-ΔK-S/E mutant peptide has a lesser or equal inhibitory effect than the wild-type peptide in the absence and presence of EGF, respectively. Stronger inhibitory effect was observed with the myristoylated wild-type peptide, while the W/E-ΔK-S/E mutant peptide was less effective both in the absence and presence of EGF (Figure 6B and Suppl. Figure S4).

### 2.4. Effect of W-7/W-12 and Grb7-derived peptides on cell invasiveness

The artificial wound healing assay has the difficulty of measuring cell migration with the interference of cells undergoing proliferation, a process that was clearly observed in the videos taken during 48-h time-lapse microscopy. Therefore, we decided to test the effect of the non-myristoylated and myristoylated peptides in a Transwell® system, which measures the transmigration of the cells across a porous membrane. This method allows to test the invasiveness of the tumor cells, as they move via a diapedesis-like process across 8 μm pores in the membrane. Figure 7A,B shows that the non-myristoylated wild-type peptide has a significant inhibitory effect, while the inhibition was weaker using the W/E-ΔK-S/E mutant peptide. Moreover, both myristoylated peptides show far stronger inhibitory effect than their non-myristoylated counterparts. In contrast, the CaM antagonists W-7 and W-12 only slightly inhibited cell invasiveness.

### 2.5. Effect of W-7/W-12 and Grb7-derived peptides on cell attachment

Cell migration requires, among other processes, the rearrangement of the cytoskeleton and the sequential attachment/detachment of focal adhesions to the extracellular matrix at the front leading edge and the rear trailing end of the cell, respectively [52]. We tested the adhesion capacity of A431 cells subjected to treatment with the different Grb7-derived myristoylated and non-myristoylated peptides and W-7/W-12 during different times using two different methods: detaching cells with the standard trypsin/ethylenediaminetetraacetic acid (EDTA) solution employed in cell culture (Figure 8A), and removing $Ca^{2+}$ from the medium using the chelating agent EGTA (Figure 8B). Surprisingly, it was shown that the myristoylated and non-myristoylated wild-type and W/E-ΔK-S/E mutant peptides strongly diminished the capacity of both treatments to detach cells from the culture plates, although the non-myristoylated form of these peptides was in general more efficient in preventing cell detachment than the myristoylated counterparts. Moreover, the W/E-ΔK-S/E mutant peptide was less efficient than the wild-type peptide in preventing cell detachment. In contrast, W-7 and W-12 have little effect in preventing cell detachment with trypsin/EDTA (Figure 8A), and only partially using EGTA (Figure 8B).

We also tested the expression of vinculin as a marker of focal adhesions using immunocytochemistry. Suppl. Figure S5 shows that treating the cells with the wild-type non-myristoylated peptide induced the disappearance of vinculin from focal adhesions. However, the W/E-ΔK-S/E mutant peptide and the CaM antagonists W-7/W-12, did not inhibit vinculin expression in focal adhesions. Moreover, the treatment with the wild-type peptide, the W/E-ΔK-S/E mutant peptides and W-7, but not with W-12, also induced a significant increase in the number of filopodia in the cells, as observed labeling the actin cytoskeleton with Alexa Fluor® 546-phalloidin (Suppl. Figure S5). This suggests a massive rearrangement of the cytoskeleton induced by these treatments.

## 3. Discussion

CaM-binding proteins could have, among others, IQ motifs (with general sequence [I,L,V]QxxxRxxx[R,K]) for $Ca^{2+}$-independent or $Ca^{2+}$-dependent CaM binding, or 1-5-8-14, 1-8-14, 1-5-8, 1-5-10 and 1-5-16 motifs, in reference to the position of conserved hydrophobic residues, for $Ca^{2+}$-dependent CaM binding [53, 54, 55]. The proposal of O'Neil and DeGrado [36] assigned great relevance for CaM-binding sites with an uneven distribution of hydrophobic and positively charged amino acid residues at opposed sides of an α-helix forming the CaM-BD of the target protein. The wild-type peptide used in this study shows this distribution in a helical

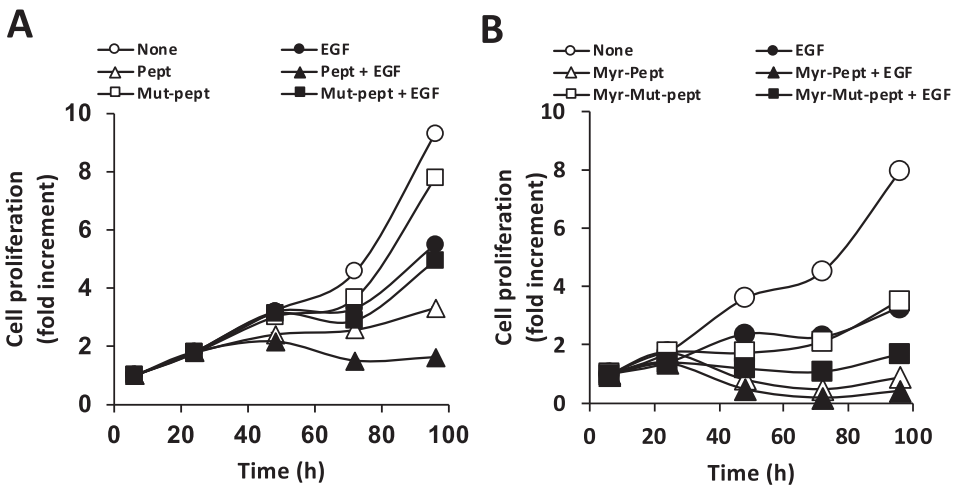


**Figure 4.** Effect of the peptides on cell proliferation. Cells ($10^5$) were seeded in the presence of 0.5 % (v/v) FBS, and treated with 10 nM EGF where indicated. After 24 h 20 μg/ml of the following peptides were added: (*A*) wild-type peptide (*Pept*) or W/E-ΔK-S/E mutant peptide (*Mut-pept*); (*B*) myristoylated wild-type peptide (*Myr-pept*) or myristoylated W/E-ΔK-S/E mutant peptide (*Myr-Mut-pept*). Controls in the absence of peptides (*None*) and the presence of 0.2% (v/v) DMSO (vehicle) were included. Cell proliferation was measured by Crystal Violet staining as described in the Experimental section. The plot represents the mean ± SEM (n = 3) fold increment proliferation at the indicated times. Error bars were smaller than the symbols.

projection which correlates with its CaM-binding property. The crystal structure of the full-length Grb7 has not been described so far, and therefore the conformation of the CaM-BD, located in the proximal region of its pleckstrin homology (PH) domain [15], is unknown. However, the structure of the Ras-associating (RA)-PH domains of the Grb7 family member protein Grb10 shows that the CaM-BD is a β-strand [56]. Therefore, by analogy the secondary structure of the CaM-BD of Grb7 could be as well a β-strand. Transitions of β-strand to α-helix are known to occur in proteins [57], as for example in amyloid peptides in Alzheimer [58] and the prion protein in scrapie [59], but it is not known whether a similar β-strand/α-helix transition occurs in the CaM-BD of Grb7 during $Ca^{2+}$/CaM binding. This is a possibility of interest to be further studied in the future. The distribution of hydrophobic and positively charged amino acid residues at opposed sides of an α-helix does not appear to be, however, a mandatory requirement for CaM-binding. We opted to prepare a mutant peptide with two acidic residues, respectively replacing a prominent hydrophobic tryptophan and a serine residue, and deleting a basic lysine residue. These modifications do not prevent CaM-binding, but they appear to be responsible for a lower inhibitory capacity of the W/E-ΔK-S/E mutant peptide in the cell functions under study, particularly in cell proliferation.

In previous studies we demonstrated that cell-permeable myristoylated and acetylated peptides corresponding to the CaM-BD of MLCK inhibited the association of Grb7 to membranes [15], and a variant cell-permeable peptide corresponding to the CaM-BD of the EGFR inhibited the EGF-dependent activation of the receptor as well as cell proliferation [26].

In this work, we demonstrate that a peptide derived from the CaM-BD of Grb7 inhibited the proliferation, migration and invasiveness of A431 tumor cells in the absence and presence of EGF, and that the W/E-ΔK-S/E mutant peptide also has inhibitory effects, albeit in lower degree. As the wild-type and W/E-ΔK-S/E mutant peptides both bind CaM in a $Ca^{2+}$-facilitated manner, it is likely that the mechanism of action of these peptides is due to the sequestration of intracellular CaM. Nevertheless, the interaction of the peptide with CaM not necessarily occurs with equal affinity, and/or in the same manner (e.g. implicating different hydrophobic residues in the EF-hands of the two globular lobes and/or the central flexible linker). This could result in the inactivation of CaM with different efficiencies, or even without affecting the capacity of CaM to regulate some CaM-binding protein targets when forming a CaM/peptide complex. Furthermore, we demonstrated that the specific order of amino acids in the CaM-BD sequence of Grb7 is not the key factor for CaM binding, as a peptide with the scrambled sequence FRSRCKLRKLFWFR efficiently bound CaM and presented inhibitory activity on the cellular functions under study (*results not shown*). This suggests that other factors such as the basic and/or hydrophobic nature of the amino acids in the peptide may be the key factor for CaM binding.

Adding a myristoyl group to the N-terminus of these peptides further enhanced their inhibitory actions, consistent with their expected increase in cell permeability. Moreover, the myristoylated peptides were in general equal or more efficient than the high-affinity CaM antagonist W-7 inhibiting these processes. The relative potency of the different myristoylated and non-myristoylated peptides, and the high- and low-affinity CaM antagonists W-7 and W-12, respectively, on different cellular functions suggests that the CaM-dependent systems implicated in the signaling pathways controlling these processes may have components with different affinities for CaM. It is expected that a system with high affinity for CaM could adequately function even when a large fraction of intracellular CaM is sequestered, while the functionality of a system with low affinity for CaM could be seriously compromised in the same experimental conditions when the available level of intracellular active CaM diminishes below a certain threshold.

The non-myristoylated and myristoylated peptides tested enhanced to different extent the adhesion of the cells to its substrate, almost totally preventing or strongly diminishing the efficiency of trypsin/EDTA treatment or $Ca^{2+}$ removal with EGTA to detach cells from the plate. As EGTA treatment has a similar effect than trypsin/EDTA treatment, this excludes the possibility that the action of the peptides was due to inhibition of the protease. We detected the disappearance of vinculin expression located at focal adhesions in cells treated with the wild-type peptide but not with the W/E-ΔK-S/E mutant peptide or W-7/W-12. This suggests that the mechanism by which the peptides enhance the attachment capacity of the cells to the substrate is unrelated to the presence of vinculin in focal adhesions. Also, the enhanced adhesion of the cells treated with the peptides is consistent with their decreased migratory capacity, suggesting that the peptides may disrupt the attachment/detachment cycle of integrins in focal adhesions during cell migration [52], and/or CaM-dependent systems implicated in cell migration, such as Grb7 [15], c-Src [60] and phosphoinositide 3-kinase [61, 62]. However, this applies to cells migrating in a two-dimensional surface, but not to cells moving in three dimensions, where focal adhesions are not involved [63]. Therefore, it is possible that the role of focal adhesions during the migration of cells across a porous membrane by a diapedesis-like mechanism may be negligible or dispensable. This suggests that the inhibitory action of the peptides observed using the Transwell® assay system, where two-dimensional migration is unnecessary, could correspond to their action on CaM-dependent systems implicated in other processes such as cytoskeleton reorganization, where the scaffold protein IQGAP1 (IQ motif-containing GTPase activating protein 1), and the small G proteins Cdc42, and Rac1 play important roles [24, 64, 65, 66].

CaM antagonists, including W-7, are well-known agents that inhibit cell proliferation [23, 50], and it has been shown that W-7 inhibits

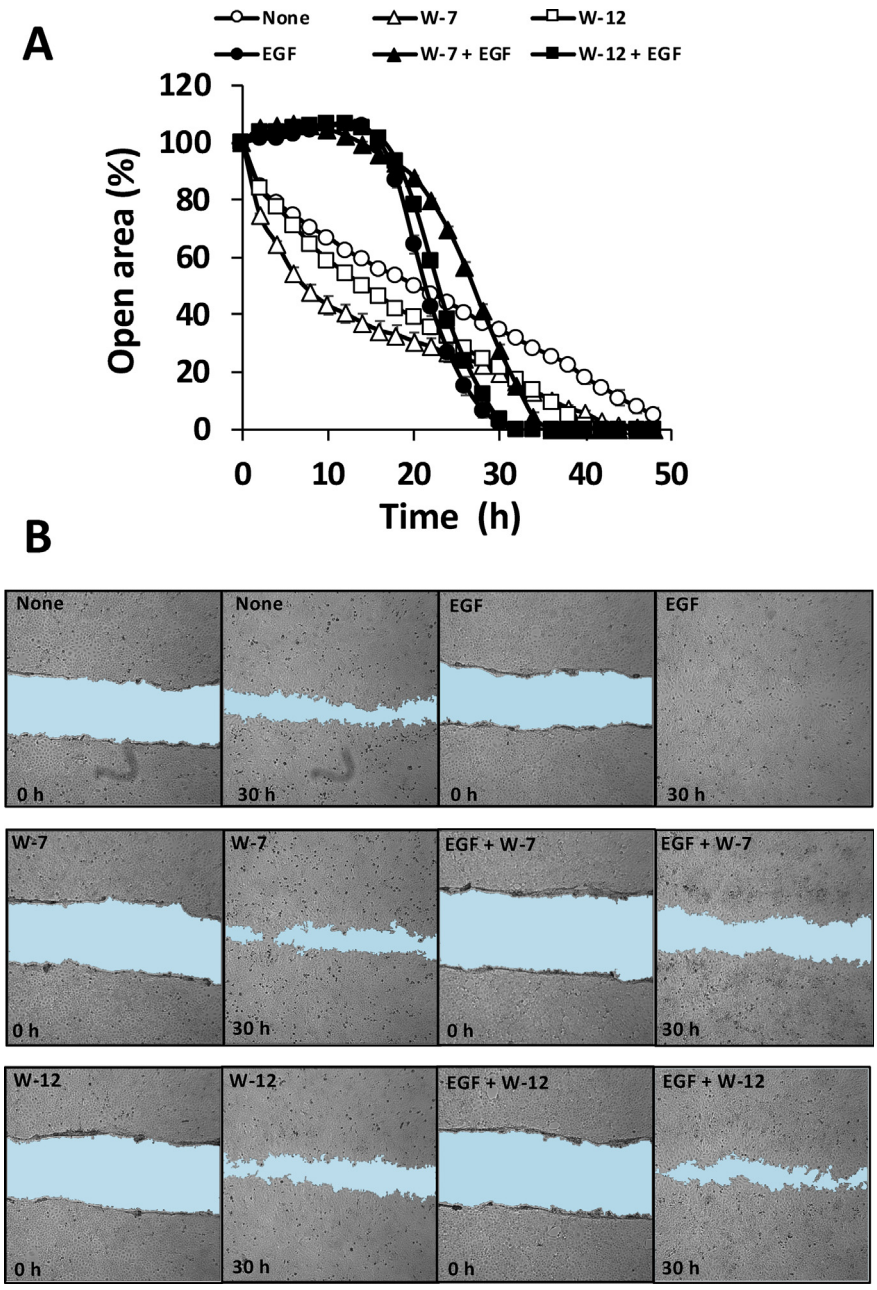


**Figure 5.** Effect of W-7/W-12 on cell migration. Cells were grown to confluency in the presence of 10 % (v/v) FBS and an artificial wound was done in the cell layer as described in the Experimental section. The cells were treated in the absence and presence of 10 nM EGF, 20 μM W-7 and 20 μM W-12 as indicated, the closing of the wound was monitored in a time-lapse microscope and photographs taken every 2 h are shown. The control in the absence of inhibitors (*None*) was treated with 0.4% (v/v) DMSO (vehicle). The plot (*A*) represents the mean ± SEM (n = 3) percent open area of the wounds at different times. Error bars are shown if larger than the symbols. Representative photographs of the wounds (*B*) in the absence (*None*) and presence of W-7, W-12 or EGF at 0 h and 30 h are shown. The open area of the wounds is highlighted in blue for clarity.

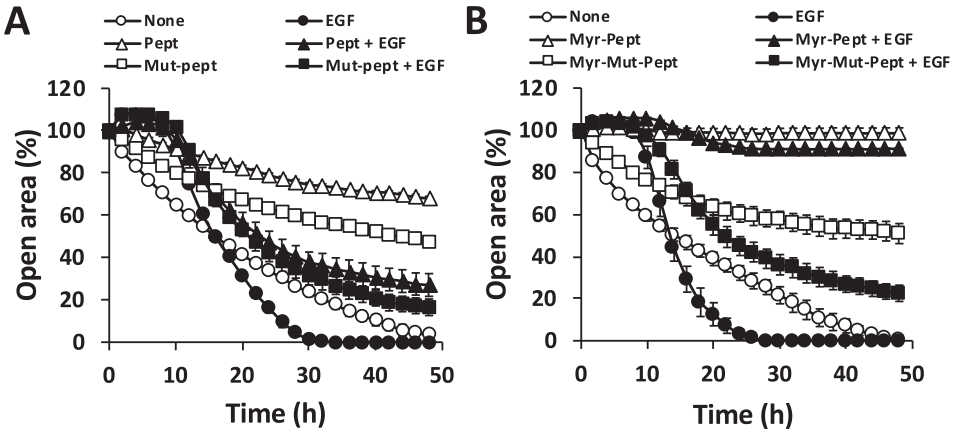


**Figure 6.** Effect of the peptides on cell migration. Cells were grown in the presence of 10 % (v/v) FBS to confluency and an artificial wound was done in the cell layer as described in the Experimental section. The cells were treated in the absence and presence of 10 nM EGF and 20 μg/ml of the following peptides: (*A*) wild-type peptide (*Pept*) or W/E-ΔK-S/E mutant peptide (*Mut-pept*); (*B*) myristoylated wild-type peptide (*Myr-pept*) or myristoylated W/E-ΔK-S/E mutant peptide (*Myr-Mut-pept*). The closing of the wound was monitored in a time-lapse microscope and photographs taken every 2 h. The control in the absence of peptides (*None*) was treated with 0.2% (v/v) DMSO (vehicle). The plots represent the mean ± SEM (n = 3) percent of open area of the wounds at different times. Error bars are shown if larger than the symbol.

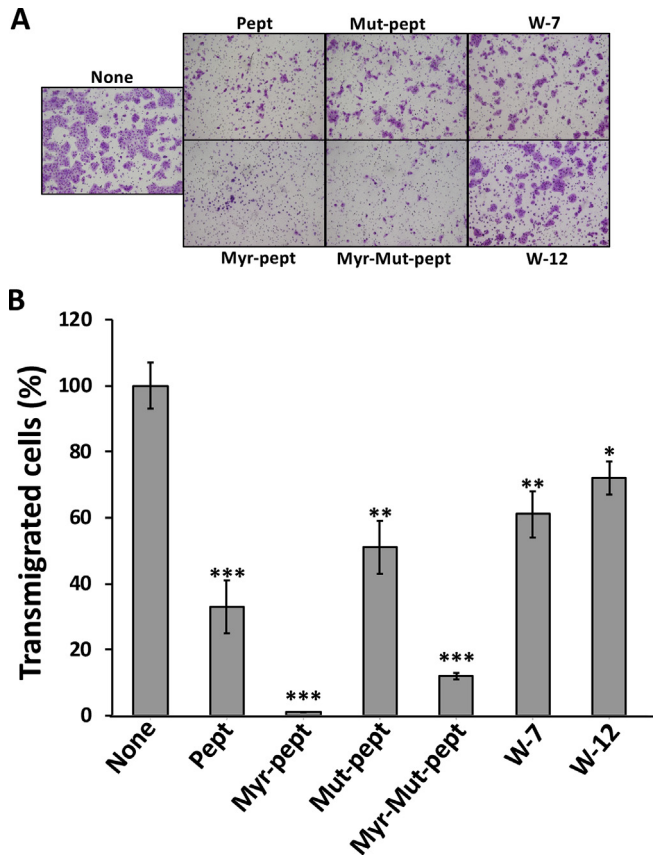


**Figure 7.** Effect of W-7/W-12 and the peptides on cell invasiveness. (*A*) Cells were seeded (1–1.5 × $10^5$) in Transwell® inserts as described in the Experimental section in the presence of 10% (v/v) FBS and incubated in the absence (*None*) and presence of 20 μg/ml wild-type peptide (*Pept*), 20 μg/ml myristoylated wild-type peptide (*Myr-pept*), 20 μg/ml W/E-ΔK-S/E mutant peptide (*Mut-pept*), 20 μg/ml myristoylated W/E-ΔK-S/E mutant peptide (*Myr-Mut-pept*), 20 μM W-7 and 20 μM W-12 as indicated. The control in the absence of inhibitors (*None*) was treated with 0.4% (v/v) DMSO (vehicle). The membranes were processed and stained as described in the Experimental section 24 h after seeding. (*B*) The plot represents the mean ± SEM (n = 6) percent of transmigrated cells across the membrane in the different conditions as indicated. Statistically significant differences were calculated using the Student's *t*-test (*p < 0.05, **p < 0.01 and ***p < 0.001).

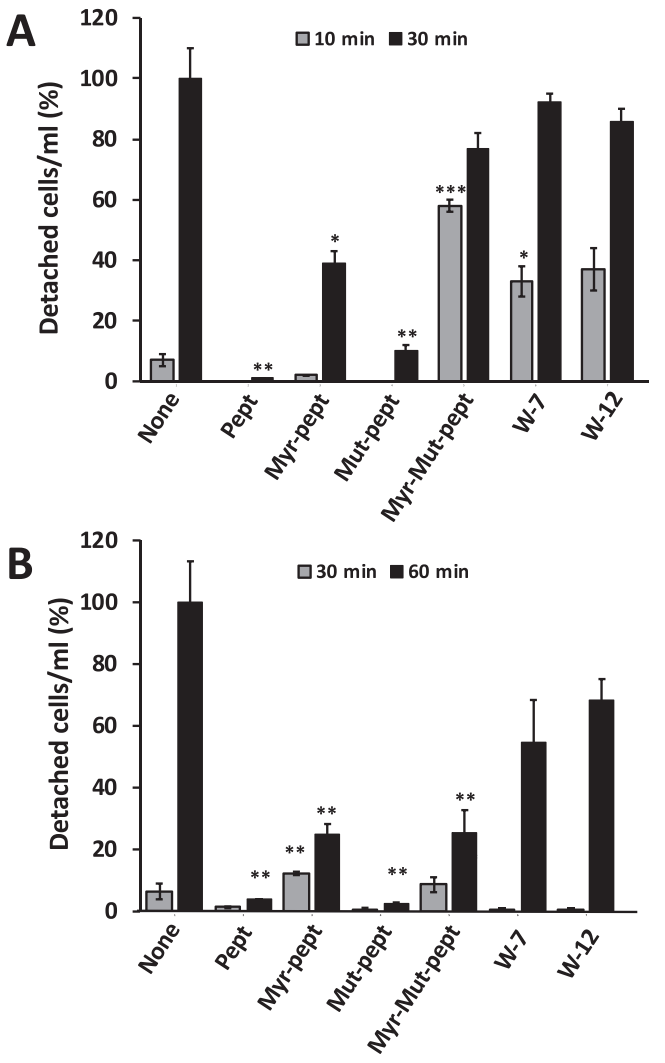


**Figure 8.** Effect of the peptides and W-7/W-12 on cell adhesion. Cells were seeded ($10^6$) and grown to confluency in the presence of 10% (v/v) FBS and treated overnight with 20 μg/ml wild-type peptide (*Pept*), 20 μg/ml myristoylated wild-type peptide (*Myr-pept*), 20 μg/ml W/E-ΔK-S/E mutant peptide (*Mut-pept*) and 20 μg/ml myristoylated W/E-ΔK-S/E mutant peptide (*Myr-Mut-pept*), 20 μM W-7 and 20 μM W-12 as indicated. The control in the absence of inhibitors (*None*) was treated with 0.4% (v/v) DMSO (vehicle). Thereafter, cells were treated with a trypsin/EDTA solution (*A*) or 1 mM EGTA (*B*) as indicated in the Experimental section. The mean ± SEM (n = 3) percent of detached cells was determined at the indicated times. Statistically significant differences were calculated using the Student's *t*-test (*p < 0.05, **p < 0.01 and ***p < 0.001).

EGF-dependent but not basal EGF-independent proliferation of hepatocarcinoma cells [67]. This suggests that a CaM-dependent signaling system is specifically implicated in EGF-mediated proliferation, in agreement with the positive regulatory role that CaM plays on the ligand-dependent activation of the EGFR [34, 41] and the inhibitory effect exerted by a cell-permeant variant peptide corresponding to the CaM-BD of the EGFR [26]. In this study, we demonstrate that W-7, and to a much lesser extent W-12, have inhibitory effects on EGF-dependent cell migration while activating EGF-independent cell migration, suggesting different signaling pathways are implicated in these distinct migratory processes. Analyzing the results obtained, it is important to consider that W-7 has other effects in addition to its capacity to antagonize CaM action. Thus, it has been reported that this agent, besides to the expected inhibition of CaM-dependent kinases, also inhibits other kinases [68], underscoring the complexity in analyzing phenomena in living cells treated with these agents.

The paradoxical inhibitory action of EGF on cell proliferation observed in cells overexpressing EGFR, as is the case in A431 cells [33], is mediated by high concentrations of EGF (>1 nM) that induces a sharp and transient activation of the MAPK pathway, in contrast to a sustained activation of this pathway at lower EGF concentration (<0.1 nM) that usually results in a proliferative response [44]. The EGF-mediated inhibitory action in this cell line requires Stat1 activation [45], and a sustained increase of the cell cycle inhibitor $p21^{Cip1/Waf1}$ [69]. In agreement with these results, we observed a strong inhibitory action of 10 nM EGF on cell proliferation and colonies formation in cells grown in soft agar. We used this concentration because it was very efficient at inducing cell migration, and we wished to standardize a constant concentration in the analysis of the effect of the peptides on the different cellular functions under study. We demonstrated that the EGF concentration used does not prevent the effect of the inhibitory peptides. The delayed action of EGF on the initiation of cell migration (11.5 ± 1.4 h, n = 9) is consistent with the required rearrangement of the cytoskeleton, responsible as well for the described EGF-dependent cell retraction [70], and the observed initial enlargement of the width of the wound open area during the lag phase occurring before initiation of cell migration.

The treatment of cells with TAMRA-labeled peptides was useful to directly visualize internalization of non-myristoylated peptides into the

cells. However, in contrast to treatment with the different non-TAMRA-labeled peptides, where the cells are viable for at least during 48 h, the cells treated with the TAMRA-peptides underwent massive blebbing in approximately 30 min under the microscope. This suggests the initiation of apoptosis, a process that was not observed with free TAMRA. This phenomenon may be due to the toxic effect of the internalized fluorescent probe and/or the combined action of the fluorescent probe attached to the peptides plus the intensity of the laser used in the microscope.

The mechanism of internalization of the peptides into the cell is unknown. This could occur by pinocytosis and/or direct binding to the plasma membrane in the case of the myristoylated peptides and subsequent internalization by a flip-flop mechanism. The myristoylated peptides could remain docked at the inner face of the membrane or could be demyristoylated upon action of intracellular deacylases, as demonstrated in multiple proteins, as for example the myristoylated alanine-rich C kinase substrate [71] and K-Ras4a [72], releasing in our case the free peptides to the cytosol and/or their distribution to other intracellular compartments. Our experiments show that the TAMRA-labeled peptides remain in the plasma membrane and in the membrane of intracellular vesicles and other intracellular structures after a long period of exposure time. Although we cannot totally exclude it, is unlikely that the fluorescent probe could play a major role in membrane attachment and/or internalization of the TAMRA-labeled peptides, as free TAMRA does not significantly enter in the cells.

Grb7 is able to undergo dimerization [21, 73, 74, 75], as is the case of other Grb7 family members Grb10 [76,77] and Grb14 [78], or higher order self-association, as tetramerization has been shown to occur in Grb10 [76]. The SH2 domain of these proteins plays a prominent role in the dimerization process, and proposed models for Grb7 dimerization suggest that the SH2 domain interacts with the RA and PH domains of the protein, either by side-to-side interaction or by tail-to-head interaction, maintaining the protein inactive, and this inactivation is released upon FAK-mediated phosphorylation [21]. As the CaM-BD of Grb7 is located in the proximal region of the PH domain [15], there is the possibility that the Grb7-derived wild-type peptides under study could act as a decoy interacting with the SH2 domain of the protein preventing Grb7 binding to the phospho-Tyr residues of active EGFR, ErbB2 or other tyrosine kinase receptors blocking further signaling [4]. However, this seems unlikely as our lab demonstrated that Grb7Δ, a mutant lacking the CaM-BD, tends to spontaneously form dimers even in denaturing gels [79].

CaM is known to bridge different or identical proteins forming homo or heterodimers [80], although is not known whether CaM facilitates Grb7 dimerization. Nevertheless, if this were the case, sequestration of intracellular CaM by the peptides derived from the CaM-BD of Grb7 should also weaken, not enhance, Grb7 dimerization, facilitating FAK-mediated phosphorylation and activation of the protein. Overall, these observations suggest that is doubtful that the observed inhibitory action of the peptides could be due to their direct action on the Grb7 protein.

Whether or not the peptides described in this work could have any anti-tumoral activity *in vivo* is something to be investigated in the future. Nevertheless, is important to consider that they could equally block the function of multiple CaM-dependent systems required for the viability of normal cells. Therefore, a more suitable therapeutic strategy to be explored in this field could be to directly target the CaM-BD of CaM-binding proteins that specifically are overexpressed and/or altered in tumor cells, such as Grb7, EGFR, ErbB2 and K-RasB, among others, as we have previously proposed [23, 26].

## 4. Experimental section

### 4.1. Reagents

Custom-designed peptides (>95% purity) were synthesized by Wuxi Nordisk Biotech Ltd. (Wuxi, China) and Schafer-N (Copenhagen, Denmark). Rabbit monoclonal anti-EGFR antibody (clone E114, IgG isotype) made against a peptide corresponding to the C-terminus of the human protein was obtained from Abcam; anti-vinculin Alexa Fluor® 488 mouse monoclonal antibody (clone 7F9, $IgG1_{\kappa}$ isotype) made against the smooth muscle protein from human uterus, Alexa Fluor® 546-phalloidin, and Prolong® Diamond Antifade Mountant medium were obtained from Invitrogen. Mouse monoclonal anti-Grb7 N-20 antibody made against a peptide corresponding to the N-terminus of the human protein (clone A-12, $IgG_{2a\kappa}$ isotype light chain) and mouse anti-rabbit IgG horseradish peroxidase (HRP)-conjugated secondary antibody (sc-2357) were purchased from Santa Cruz Biotechnology Inc. Mouse monoclonal anti-GAPDH antibody (clone GA1R, IgG1 isotype) made against a recombinant protein was obtained from Thermo Fischer Scientific. Transwell® inserts (24-well, polyethylene terephthalate membrane with 8 μm pore size) were from Falcon. Dulbecco's modified Eagle's medium (DMEM), trypsin/EDTA, L-glutamine and FBS were obtained from Gibco; Anti-mouse IgG (whole molecule) HRP-conjugated secondary antibody (A9044), phenyl-Sepharose 6 (fast-flow), dansyl chloride, glutaraldehyde, *N,N,N′,N′*-tetramethylethylenediamine, Triton X-100, Fast Green FC and Crystal Violet were purchased from Sigma-Aldrich; polyvinylidene difluoride (PVDF) membranes, the mouse monoclonal anti-phosphotyrosine antibody (clone 4G10, $IgG_{2b\kappa}$ isotype) made against phosphotyramine-KLH (keyhole limpet hemocyanin), fibronectin, dimethyl sulfoxide (DMSO), acrylamide and EGF were from Merck Millipore; W-7 and W-12 were obtained from Calbiochem or Abcam, and 5(6)-TAMRA was from Novabiochem®. The Diff-Quik staining kit was from Medion Diagnostics AG, bovine serum albumin (BSA) was from Nzytech and the enhanced chemiluminescence (ECL) kit was purchased from GE Healthcare-Amersham. Ammonium persulfate was from Bio-Rad, and gentamicin from Normon. The mycoplasma gel detection kit was obtained from Biotools B&M Labs S.A. The pETCM vector for recombinant CaM expression was kindly provided by Prof. Nobuhiro Hayashi from the Institute for Comprehensive Medical Science, Fujita Health University, Japan. Other reagents were of analytical grade.

### 4.2. Cell culture

Human epidermoid carcinoma A431 cells (ATCC® CRL-1555™) were grown in DMEM supplemented with 2 mM L-glutamine, 40 μg/ml gentamicin and 10% (v/v) FBS at 37 °C in a 5% (v/v) $CO_2$ atmosphere. Cells were tested to be mycoplasma free by PCR amplifying a conserved region of the 16S ribosome RNA using the mycoplasma detection kit of Biotools following instructions of the manufacturer.

### 4.3. Calmodulin dansylation and peptides binding

Recombinant rat CaM was expressed in *Escherichia coli* (strain BL21) and purified using a phenyl-Sepharose affinity chromatography column as previously described [81, 82]. The samples were dialyzed against ultrapure water and CaM was dansylated at room temperature with dansyl chloride as previously described [83]. Binding of the wild type and W/E-ΔK-S/E mutant peptides to CaM was determined adding increasing concentrations (0.1–12 μg/ml) of the peptides to 30 μg/ml dansyl-CaM in 1 ml of deionized water containing 10 mM $CaCl_2$ or 20 mM EGTA using a Horiba Jobin Yvon Fluoromax-4 spectrofluorometer (Kyoto, Japan) exciting the sample at 340 nm and measuring the emission spectra at 450–600 nm.

### 4.4. TAMRA-peptides internalization assay

The internalization of the wild type and W/E-ΔK-S/E mutant peptides conjugated at the N-terminus with 5(6)-TAMRA was monitored by two methods: flow cytometry and confocal microscopy. For cytometry analysis, $10^6$ cells were seeded in 60 mm dishes in DMEM supplemented with 10% (v/v) FBS. Six hours thereafter, fresh serum-free medium was added containing the different TAMRA-peptides (20 μg/ml) as indicated in the legend of the figures and the cells were incubated at 37 °C overnight.

Controls in the absence of peptides and 0.2% (v/v) DMSO (vehicle) were included. Cells were washed with fresh medium, detached with trypsin/EDTA, centrifugated at 1230 x *g* during 5 min and aliquoted in appropriated cytometry tubes. The samples were analyzed ($10^4$ cells) in a BD-FACSCanto™ II cytometer using a 488 nm excitation laser. For confocal microscopy analysis, $2.5 \times 10^5$ cells were seeded in a 35 mm imaging dishes with a polymer coverslip bottom (ibidi Gmbl, Germany) in DMEM supplemented with 10% (v/v) FBS. Six hours thereafter, fresh serum-deprived medium was added containing the different TAMRA-peptides (20 μg/ml) and the cells were incubated as indicated in the legend of the figures. Cells were gently washed with fresh medium and photographs of different z-planes were taken every 0.8 μm using a spectral confocal microscope LSM710 (Zeiss) with a 63x Plan-APOCHROMAT objective using the 561 nm laser and white light. Controls using free TAMRA (1.7 μM) were included with both techniques.

### 4.5. EGFR activation assays

Cells were seeded in DMEM supplemented with 10% (v/v) FBS ($2 \times 10^6$ cells in 60 mm dishes). Six hours thereafter the cells were serum deprived overnight. Thereafter, the cells were incubated 15 min with the myristoylated and non-myristoylated peptides (50 μg/ml) dissolved in DMSO and the EGFR was activated with 10 nM EGF during 5 min at room temperature. Controls in the absence of peptides and 1% (v/v) DMSO (vehicle) were included. The reaction was swiftly arrested with ice-cold 10% (v/v) trichloroacetic acid as previously described [41], and the samples were processed for sodium dodecyl sulfate-polyacrylamide gel electrophoresis (SDS-PAGE) and Western blot.

### 4.6. SDS-PAGE and Western blot

Proteins were separated by SDS-PAGE [84] using 8% (w/v) polyacrylamide slab gels, electro-transferred to a PVDF membrane, fixed 10 min with 0.2% (v/v) glutaraldehyde, and transiently stained with 0.1% (w/v) Fast Green FCF to ascertain correct loading using standard procedures. The PVDF membranes were blocked with 5% (w/v) bovine serum albumin or 5% (w/v) fat-free powdered milk according to the instructions of the antibodies' manufacturers, and incubated overnight at 4 °C with the primary antibodies (1/2000 dilution) and for 1 h at room temperature with the secondary antibodies coupled to HRP (1/5000 dilution). The bands were visualized with the ECL reagents following instructions of the manufacturer.

### 4.7. Cell proliferation assays

Cells were seeded in DMEM in the presence of 0.5% (v/v) FBS and in the absence and presence of 10 nM EGF ($10^5$ cells in 60 mm dishes). The myristoylated and non-myristoylated peptides (20 μg/ml) and the CaM antagonists W-7/W-12 (15 μM) dissolved in DMSO were added 24 h after seeding and cell attachment. Controls in the absence of peptides or CaM antagonists containing 0.2–0.3% (v/v) DMSO (vehicle) were included. At the indicated times the cells were washed with phosphate buffer saline (137 mM NaCl, 2.7 mM KCl, 10 mM $Na_2HPO_4$, 1.8 mM $KH_2PO_4$, pH 7.4), fixed for 10 min with 1% (v/v) glutaraldehyde and stained with 0.1% (w/v) Crystal Violet. After extraction of the dye with 10% (v/v) acetic acid its absorbance was measured spectrophotometrically as previously described [85] at 600 nm after subtracting the background absorbance at 450 nm.

### 4.8. Anchorage-independent growth assays

A cell suspension in DMEM in the absence or presence of 10% (v/v) FBS and 10 mM NaOH-Hepes (pH 7.5) was mixed with warm liquified 0.3% (w/v) agarose to form an upper layer that was seeded over a lower layer of 0.5% (w/v) agarose in the absence and presence of 10% (v/v) FBS and 10 mM NaOH-Hepes pH 7.5 ($10^5$ cells in 60 mm dishes). Cells were replenished every 72–96 h with fresh medium (400 μl per dish) in the absence and presence of the CaM antagonists W-7 (20 μM) and W-12 (25 μM) dissolved in DMSO and other reagents indicated in the legend of the figures. Controls in the absence of CaM antagonists containing 0.4% (v/v) DMSO (vehicle) were included. After 14 days of growth, pictures of the plates were taken in an Observer.Z1 microscope with a Cascade 1K camera and a 4x objective. Colonies ≥60 μm diameter were counted using the ImageJ digital image processing computer software.

### 4.9. Artificial wound healing assays

Cells were seeded ($4 \times 10^5$-$10^6$ cells in p6 multi-well plates) in DMEM supplemented with 10% (v/v) and grown until confluence. The monolayer was scratched with a 200 μl pipette tip and washed twice with serum-deprived medium in order to remove the floating cells. Fresh serum-deprived medium was added with the myristoylated and non-myristoylated peptides (20 μg/ml) and the CaM antagonists W-7/W-12 (20 μM) dissolved in DMSO and other reagents indicated in the legend of the figures. Controls in the absence of peptides or W-7/W-12 and 0.2–0.4% (v/v) DMSO (vehicle) were included. The wound closure was monitored by time-lapse microscopy during 48 h taking photographs every 2 h with an Observer.Z1 microscope with a Cascade 1K camera and a 4x objective inside an environmental controlled chamber at 37 °C in a 5% (v/v) $CO_2$ atmosphere. The open area of the wound during migration was quantified with the ImageJ digital image processing computer software.

### 4.10. Cell invasiveness assay

Cell motility and invasiveness were analyzed by the Boyden Chamber method using Transwell® inserts. Cells were seeded ($1–1.5 \times 10^5$ cells per insert) in the upper chamber in serum-free DMEM in the absence or presence of the myristoylated and non-myristoylated peptides (20 μg/ml) and the CaM antagonists W-7/W-12 (20 μM) dissolved in DMSO and other reagents indicated in the legend of the figures. Controls in the absence of peptides and 0.2–0.4% (v/v) DMSO (vehicle) were included. The lower chamber was filled with DMEM supplemented with 10% (v/v) FBS in the absence or presence of the reagents as indicated above. The cells on top of the upper face of the porous membrane of the inserts were removed 24 h thereafter with a cotton swab, and the cells migrated to the bottom face of the membrane were fixed and stained with Diff-Quik reagents following the manufacturer procedure. Seven pictures of evenly spaced fields in the bottom face of the membrane were taken in bright-field with a Plan-NEOFLUAR 10x objective in an Axiophot microscope (Zeiss) using an integrated color camera DP70 (Olympus). Completely migrated cells in which the nucleus was clearly visible were counted with the ImageJ digital image processing computer software.

### 4.11. Cell detachment assay

Cells were seeded in DMEM supplemented with 10% (v/v) FBS ($10^6$ cells in 60 mm dishes). Six hours thereafter, the myristoylated and non-myristoylated peptides (20 μg/ml) and the CaM antagonists W-7/W-12 (20 μM) dissolved in DMSO were added in a serum-deprived medium and incubated overnight. Controls in the absence of peptides and 0.2–0.4% (v/v) DMSO (vehicle) were included. Cell detachment was determined upon trypsin/EDTA treatment or extracellular calcium chelation with 1 mM EGTA during the indicated times in the figures counting the number of detached cells in aliquots at different times using a Neubauer chamber.

### 4.12. Confocal microscopy

To visualize the actin cytoskeleton and vinculin localization $5 \times 10^4$ cells were seeded in 24-multiwell plates containing fibronectin-coated coverslips. Six hours thereafter, the myristoylated and non-myristoylated peptides (20 μg/ml) and the CaM antagonists W-7/W-12

(20 μM) dissolved in DMSO were added in fresh FBS-free DMEM and incubated overnight at 37 °C in a 5% (v/v) $CO_2$ atmosphere. Controls in the absence of peptides or W-7/W-12 and 0.2–0.4% (v/v) DMSO (vehicle) were included. Cells were fixed with 4% (w/v) para-formaldehyde, permeabilized with 0.1% (v/v) Triton X-100, blocked with 5% (w/v) BSA and incubated 2 h with 20 μg/ml Alexa Fluor® 488 conjugated anti-vinculin antibody, and 40 min with Alexa Fluor® 546-phalloidin (1:66 dilution) and 4′,6-diamidine-2′-phenylindole (DAPI) (1:1000 dilution) at room temperature. The coverslips were placed faced-down on microscope slides using ProLong® Diamond Antifade mounting solution. Images were acquired with a spectral confocal microscope LSM710 (Zeiss) using a Plan-APOCHROMAT 63x oil-immersion objective focusing the planes at 0.6 μm intervals. The images were processed with the Zen2009 image acquisition software.

### 4.13. Statistics analysis

Statistics analysis was performed with the Microsoft Excel software using the unpaired two-tails Student's *t*-test. Differences were considered significant at $p < 0.05$ as indicated in the legends to the figures.

## Declarations

### Author contribution statement

Juan Alcalde, María González-Muñoz: Performed the experiments; Analyzed and interpreted the data.

Antonio Villalobo: Conceived and designed the experiments; Analyzed and interpreted the data; Wrote the paper.

### Funding statement

This work was supported by grants to AV from the Secretaría de Estado de Investigación, Desarrollo e Innovación (SAF2014-52048-R), and the Consejería de Educación, Juventud y Deportes – Comunidad de Madrid (B2017/BMD-36) involving contributions from the European Funds for Regional Development (EFRD) and the Social European Fund (SEF).

### Competing interest statement

The authors declare no conflicting interest.

### Additional information

Supplementary content related to this article has been published online at https://doi.org/10.1016/j.heliyon.2020.e03922.

## Acknowledgments

We thank Prof. Jacqueline A. Wilce from Monash University (Australia) and Dr. Gemma Ferrer from our Institute for providing reagents, Dr. Dolores Solís from the Instituto de Química Física Rocasolano - CSIC for access and assistant with the spectrofluorometer, Dr. Víctor Mayoral from our Institute for critical comments and expert assistance in some experiments, and Dr. Svetlana Panina and Prof. Martin W. Berchtold from the University of Copenhagen for useful comments to the manuscript. We also thank the technical assistance of the personnel in our microscopy core facility.

## References

[1] R.J. Daly, The Grb7 family of signalling proteins, Cell. Signal. 10 (9) (1998) 613–618.
[2] D.C. Han, T.L. Shen, J.L. Guan, The Grb7 family proteins: structure, interactions with other signaling molecules and potential cellular functions, Oncogene 20 (44) (2001) 6315–6321.
[3] T.L. Shen, J.L. Guan, Grb7 in intracellular signaling and its role in cell regulation, Front. Biosci. 9 (2004) 192–200.
[4] A. Villalobo, H. Li, J. Sánchez-Torres, The Grb7 protein family, Curr. Top. Biochem. Res. 5 (2003) 105–114.
[5] A. Walch, K. Specht, H. Braselmann, H. Stein, J.R. Siewert, U. Hopt, H. Hofler, M. Werner, Coamplification and coexpression of GRB7 and ERBB2 is found in high grade intraepithelial neoplasia and in invasive Barrett's carcinoma, Int. J. Cancer 112 (5) (2004) 747–753.
[6] Y. Wang, D.W. Chan, V.W. Liu, P. Chiu, H.Y. Ngan, Differential functions of growth factor receptor-bound protein 7 (GRB7) and its variant GRB7v in ovarian carcinogenesis, Clin. Cancer Res. 16 (9) (2010) 2529–2539.
[7] B. Ramsey, T. Bai, A. Hanlon Newell, M. Troxell, B. Park, S. Olson, E. Keenan, S.W. Luoh, GRB7 protein over-expression and clinical outcome in breast cancer, Breast Cancer. Res. Treat. 127 (3) (2011) 659–669.
[8] W.W. Bivin, O. Yergiyev, M.L. Bunker, J.F. Silverman, U. Krishnamurti, GRB7 expression and correlation with HER2 amplification in invasive breast carcinoma, Appl. Immunohistochem. Mol. Morphol. 25 (8) (2017) 553–558.
[9] H.B. Zhao, X.F. Zhang, X.L. Jia, H.B. Wang, Grb7 is over-expressed in cervical cancer and facilitate invasion and inhibit apoptosis in cervical cancer cells, Pathol. Res. Pract. 213 (9) (2017) 1180–1184.
[10] W. Jacot, M. Fiche, K. Zaman, A. Wolfer, P.J. Lamy, The HER2 amplicon in breast cancer: topoisomerase IIA and beyond, Biochim. Biophys. Acta 1836 (1) (2013) 146–157.
[11] S.W. Luoh, W. Wagoner, X. Wang, Z. Hu, X. Lai, K. Chin, R. Sears, E. Ramsey, GRB7 dependent proliferation of basal-like, HER-2 positive human breast cancer cell lines is mediated in part by HER-1 signaling, Mol. Carcinog. (2019).
[12] P.Y. Chu, T.K. Li, S.T. Ding, I.R. Lai, T.L. Shen, EGF-induced Grb7 recruits and promotes Ras activity essential for the tumorigenicity of Sk-Br3 breast cancer cells, J. Biol. Chem. 285 (38) (2010) 29279–29285.
[13] D. Pradip, M. Bouzyk, N. Dey, B. Leyland-Jones, Dissecting GRB7-mediated signals for proliferation and migration in HER2 overexpressing breast tumor cells: GTP-ase rules, Am. J. Cancer Res. 3 (2) (2013) 173–195.
[14] I. García-Palmero, P. López-Larrubia, S. Cerdán, A. Villalobo, Nuclear magnetic resonance imaging of tumour growth and neovasculature performance in vivo reveals Grb7 as a novel antiangiogenic target, NMR Biomed. 26 (2013) 1059–1069.
[15] H. Li, J. Sánchez-Torres, A.F. del Carpio, A. Nogales-González, P. Molina-Ortiz, M.J. Moreno, K. Török, A. Villalobo, The adaptor Grb7 is a novel calmodulin-binding protein: functional implications of the interaction of calmodulin with Grb7, Oncogene 24 (26) (2005) 4206–4219.
[16] O. Giricz, V. Calvo, S.C. Pero, D.N. Krag, J.A. Sparano, P.A. Kenny, GRB7 is required for triple-negative breast cancer cell invasion and survival, Breast Cancer. Res. Treat. 133 (2) (2012) 607–615.
[17] R.C. Lim, J.T. Price, J.A. Wilce, Context-dependent role of Grb7 in HER2+ve and triple-negative breast cancer cell lines, Breast Cancer. Res. Treat. 143 (3) (2014) 593–603.
[18] S. Tanaka, M. Mori, T. Akiyoshi, Y. Tanaka, K. Mafune, J.R. Wands, K. Sugimachi, A novel variant of human Grb7 is associated with invasive esophageal carcinoma, J. Clin. Invest. 102 (4) (1998) 821–827.
[19] I. García-Palmero, N. Pompas-Veganzones, E. Villalobo, S. Gioria, J. Haiech, A. Villalobo, The adaptors Grb10 and Grb14 are calmodulin-binding proteins, FEBS Lett. 591 (2017) 1176–1186.
[20] I. García-Palmero, A. Villalobo, Calmodulin regulates the translocation of Grb7 into the nucleus, FEBS Lett. 586 (10) (2012) 1533–1539.
[21] S. Siamakpour-Reihani, H.J. Argiros, L.J. Wilmeth, L.L. Haas, T.A. Peterson, D.L. Johnson, C.B. Shuster, B.A. Lyons, The cell migration protein Grb7 associates with transcriptional regulator FHL2 in a Grb7 phosphorylation-dependent manner, J. Mol. Recogn. 22 (1) (2009) 9–17.
[22] I. García-Palmero, A. Villalobo, Deletion of the calmodulin-binding domain of Grb7 impairs cell attachment to the extracellular matrix and migration, Biochem. Biophys. Res. Commun. 436 (2013) 271–277.
[23] M.W. Berchtold, A. Villalobo, The many faces of calmodulin in cell proliferation, programmed cell death, autophagy, and cancer, Biochim. Biophys. Acta 1843 (2014) 398–435.
[24] A. Villalobo, M.W. Berchtold, The role of calmodulin in tumor cell migration, invasiveness and metastasis, Int. J. Mol. Sci. 21 (2020) 765.
[25] D.W. Chan, W.W. Hui, P.C. Cai, M.X. Liu, M.M. Yung, C.S. Mak, T.H. Leung, K.K. Chan, H.Y. Ngan, Targeting GRB7/ERK/FOXM1 signaling pathway impairs aggressiveness of ovarian cancer cells, PloS One 7 (12) (2012), e52578.
[26] A. Villalobo, I. García-Palmero, S.R. Stateva, K. Jellali, Targeting the calmodulin-regulated ErbB/Grb7 signaling axis in cancer therapy, J. Pharm. Pharmaceut. Sci. 16 (2) (2013) 177–189.
[27] D. Kraskouskaya, E. Duodu, C.C. Arpin, P.T. Gunning, Progress towards the development of SH2 domain inhibitors, Chem. Soc. Rev. 42 (8) (2013) 3337–3370.
[28] C.J. Porter, J.M. Matthews, J.P. Mackay, S.E. Pursglove, J.W. Schmidberger, P.J. Leedman, S.C. Pero, D.N. Krag, M.C. Wilce, J.A. Wilce, Grb7 SH2 domain structure and interactions with a cyclic peptide inhibitor of cancer cell migration and proliferation, BMC Struct. Biol. 7 (2007) 58.
[29] N.D. Ambaye, S.C. Pero, M.J. Gunzburg, M. Yap, D.J. Clayton, M.P. Del Borgo, P. Perlmutter, M.I. Aguilar, G.S. Shukla, E. Peletskaya, M.M. Cookson, D.N. Krag, M.C. Wilce, J.A. Wilce, Structural basis of binding by cyclic nonphosphorylated peptide antagonists of Grb7 implicated in breast cancer progression, J. Mol. Biol. 412 (3) (2011) 397–411.
[30] G.M. Watson, K. Kulkarni, J. Sang, X. Ma, M.J. Gunzburg, P. Perlmutter, M.C.J. Wilce, J.A. Wilce, Discovery, development, and cellular delivery of potent and sdelective bicyclic peptide inhibitors of Grb7 cancer target, J. Med. Chem. 60 (22) (2017) 9349–9359.

[31] G.M. Watson, K. Kulkarni, R. Brandt, M.P. Del Borgo, M.I. Aguilar, J.A. Wilce, Shortened penetratin cell-penetrating peptide is insufficient for cytosolic delivery of a Grb7 targeting peptide, ACS Omega 2 (2) (2017) 670–677.

[32] D.D. Ourth, Antitumor cell activity in vitro by myristoylated-peptide, Biomed. Pharmacother. 65 (4) (2011) 271–274.

[33] A. Ullrich, L. Coussens, J.S. Hayflick, T.J. Dull, A. Gray, A.W. Tam, J. Lee, Y. Yarden, T.A. Libermann, J. Schlessinger, et al., Human epidermal growth factor receptor cDNA sequence and aberrant expression of the amplified gene in A431 epidermoid carcinoma cells, Nature 309 (5967) (1984) 418–425.

[34] P. Sánchez-González, K. Jellali, A. Villalobo, Calmodulin-mediated regulation of the epidermal growth factor receptor, FEBS J. 277 (2) (2010) 327–342.

[35] S. Tanaka, M. Mori, T. Akiyoshi, Y. Tanaka, K. Mafune, J.R. Wands, K. Sugimachi, Coexpression of Grb7 with epidermal growth factor receptor or Her2/erbB2 in human advanced esophageal carcinoma, Cancer Res. 57 (1) (1997) 28–31.

[36] K.T. O'Neil, W.F. DeGrado, How calmodulin binds its targets: sequence independent recognition of amphiphilic alpha-helices, Trends Biochem. Sci. 15 (2) (1990) 59–64.

[37] P.Y. Chu, L.Y. Huang, C.H. Hsu, C.C. Liang, J.L. Guan, T.H. Hung, T.L. Shen, Tyrosine phosphorylation of growth factor receptor-bound protein-7 by focal adhesion kinase in the regulation of cell migration, proliferation, and tumorigenesis, J. Biol. Chem. 284 (30) (2009) 20215–20226.

[38] J. Martín-Nieto, A. Villalobo, The human epidermal growth factor receptor contains a juxtamembrane calmodulin-binding site, Biochemistry 37 (1) (1998) 227–236.

[39] H. Li, A. Villalobo, Evidence for the direct interaction between calmodulin and the human epidermal growth factor receptor, Biochem. J. 362 (Pt 2) (2002) 499–505.

[40] H. Li, M.J. Ruano, A. Villalobo, Endogenous calmodulin interacts with the epidermal growth factor receptor in living cells, FEBS Lett. 559 (1-3) (2004) 175–180.

[41] H. Li, S. Panina, A. Kaur, M.J. Ruano, P. Sánchez-González, J.M. la Cour, A. Stephan, U.H. Olesen, M.W. Berchtold, A. Villalobo, Regulation of the ligand-dependent activation of the epidermal growth factor receptor by calmodulin, J. Biol. Chem. 287 (5) (2012) 3273–3281.

[42] S.R. Stateva, V. Salas, A. Benguría, I. Cossio, E. Anguita, J. Martín-Nieto, G. Benaim, A. Villalobo, The activating role of phospho-(Tyr)-calmodulin on the epidermal growth factor receptor, Biochem. J. 472 (2) (2015) 195–204.

[43] A.R. Nelson, L. Borland, N.L. Allbritton, C.E. Sims, Myristoyl-based transport of peptides into living cells, Biochemistry 46 (51) (2007) 14771–14781.

[44] N. Chajry, P.M. Martin, G. Pages, C. Cochet, K. Afdel, Y. Berthois, Relationship between the MAP kinase activity and the dual effect of EGF on A431 cell proliferation, Biochem. Biophys. Res. Commun. 203 (2) (1994) 984–990.

[45] J.F. Bromberg, Z. Fan, C. Brown, J. Mendelsohn, J.E. Darnell Jr., Epidermal growth factor-induced growth inhibition requires Stat1 activation, Cell Growth Differ. 9 (7) (1998) 505–512.

[46] H. Hidaka, T. Tanaka, Naphthalenesulfonamides as calmodulin antagonists, Methods Enzymol. 102 (1983) 185–194.

[47] H. Hidaka, M. Asano, T. Tanaka, Activity-structure relationship of calmodulin antagonists, Naphthalenesulfonamide derivatives, Mol. Pharmacol. 20 (3) (1981) 571–578.

[48] M.L. Veigl, W.D. Sedwick, J. Niedel, M.E. Branch, Induction of myeloid differentiation of HL-60 cells with naphthalene sulfonamide calmodulin antagonists, Cancer Res. 46 (5) (1986) 2300–2305.

[49] M.L. Veigl, R.E. Klevit, W.D. Sedwick, The uses and limitations of calmodulin antagonists, Pharmacol. Ther. 44 (2) (1989) 181–239.

[50] H. Hidaka, Y. Sasaki, T. Tanaka, T. Endo, S. Ohno, Y. Fujii, T. Nagata, N-(6-aminohexyl)-5-chloro-1-naphthalenesulfonamide, a calmodulin antagonist, inhibits cell proliferation, Proc. Natl. Acad. Sci. U. S. A. 78 (7) (1981) 4354–4357.

[51] J.W. Wei, R.A. Hickie, D.J. Klaassen, Inhibition of human breast cancer colony formation by anticalmodulin agents: trifluoperazine, W-7, and W-13, Cancer Chemother. Pharmacol. 11 (2) (1983) 86–90.

[52] B. Wehrle-Haller, B.A. Imhof, Actin, microtubules and focal adhesion dynamics during cell migration, Int. J. Biochem. Cell Biol. 35 (1) (2003) 39–50.

[53] A.R. Rhoads, F. Friedberg, Sequence motifs for calmodulin recognition, Faseb. J. 11 (5) (1997) 331–340.

[54] M. Bähler, A. Rhoads, Calmodulin signaling via the IQ motif, FEBS Lett. 513 (1) (2002) 107–113.

[55] S.W. Vetter, E. Leclerc, Novel aspects of calmodulin target recognition and activation, Eur. J. Biochem. 270 (3) (2003) 404–414.

[56] R.S. Depetris, J. Wu, S.R. Hubbard, Structural and functional studies of the Ras-associating and pleckstrin-homology domains of Grb10 and Grb14, Nat. Struct. Mol. Biol. 16 (8) (2009) 833–839.

[57] V.V. Khrustalev, T.A. Khrustaleva, V.V. Poboinev, Amino acid content of beta strands and alpha helices depends on their flanking secondary structure elements, Biosystems 168 (2018) 45–54.

[58] S.G. Jacchieri, Study of alpha-helix to beta-strand to beta-sheet transitions in amyloid: the role of segregated hydrophobic beta-strands, Biophys. Chem. 74 (1) (1998) 23–34.

[59] M. Gasset, M.A. Baldwin, R.J. Fletterick, S.B. Prusiner, Perturbation of the secondary structure of the scrapie prion protein under conditions that alter infectivity, Proc. Natl. Acad. Sci. U. S. A. 90 (1) (1993) 1–5.

[60] S.R. Stateva, V. Salas, E. Anguita, G. Benaim, A. Villalobo, Ca2+/calmodulin and apo-calmodulin both bind to and enhance the tyrosine kinase activity of c-Src, PloS One 10 (6) (2015), e0128783.

[61] G. Wang, M. Zhang, H. Jang, S. Lu, S. Lin, G. Chen, R. Nussinov, J. Zhang, V. Gaponenko, Interaction of calmodulin with the cSH2 domain of the p85 regulatory subunit, Biochemistry 57 (12) (2018) 1917–1928.

[62] M. Zhang, H. Jang, V. Gaponenko, R. Nussinov, Phosphorylated calmodulin promotes PI3K activation by binding to the SH2 domains, Biophys. J. 113 (9) (2017) 1956–1967.

[63] E.K. Paluch, I.M. Aspalter, M. Sixt, Focal adhesion-independent cell migration, Annu. Rev. Cell Dev. Biol. 32 (2016) 469–490.

[64] A.R. Means, J.S. Tash, J.G. Chafouleas, L. Lagace, V. Guerriero, Regulation of the cytoskeleton by Ca2+-calmodulin and cAMP, Ann. N. Y. Acad. Sci. 383 (1982) 69–84.

[65] M.W. Briggs, D.B. Sacks, IQGAP1 as signal integrator: Ca2+, calmodulin, Cdc42 and the cytoskeleton, FEBS Lett. 542 (1-3) (2003) 7–11.

[66] A.J. Ridley, Rho GTPases and actin dynamics in membrane protrusions and vesicle trafficking, Trends Cell Biol. 16 (10) (2006) 522–529.

[67] B.W. Wu, Y. Wu, J.L. Wang, J.S. Lin, S.Y. Yuan, A. Li, W.R. Cui, Study on the mechanism of epidermal growth factor-induced proliferation of hepatoma cells, World J. Gastroenterol. 9 (2) (2003) 271–275.

[68] R.C. Schatzman, R.L. Raynor, J.F. Kuo, N-(6-Aminohexyl)-5-chloro-1-naphthalenesulfonamide(W-7), a calmodulin antagonist, also inhibits phospholipid-sensitive calcium-dependent protein kinase, Biochim. Biophys. Acta 755 (1) (1983) 144–147.

[69] E. Skarpen, L.E. Johannessen, K. Bjerk, H. Fasteng, T.K. Guren, B. Lindeman, G.H. Thoresen, T. Christoffersen, E. Stang, H.S. Huitfeldt, I.H. Madshus, Endocytosed epidermal growth factor (EGF) receptors contribute to the EGF-mediated growth arrest in A431 cells by inducing a sustained increase in p21/CIP1, Exp. Cell Res. 243 (1) (1998) 161–172.

[70] K.H. Sit, K.P. Wong, Induced interphase cell retraction: its reversal and EGF potentiation, Tissue Cell 21 (3) (1989) 321–333.

[71] S. Manenti, O. Sorokine, A. Van Dorsselaer, H. Taniguchi, Demyristoylation of the major substrate of protein kinase C (MARCKS) by the cytoplasmic fraction of brain synaptosomes, J. Biol. Chem. 269 (11) (1994) 8309–8313.

[72] N.A. Spiegelman, J.Y. Hong, J. Hu, H. Jing, M. Wang, I.R. Price, J. Cao, M. Yang, X. Zhang, H. Lin, A small-molecule SIRT2 inhibitor that promotes K-Ras4a lysine fatty-acylation, ChemMedChem (2019).

[73] C.J. Porter, M.C. Wilce, J.P. Mackay, P. Leedman, J.A. Wilce, Grb7-SH2 domain dimerisation is affected by a single point mutation, Eur. Biophys. J. 34 (5) (2005) 454–460.

[74] T.A. Peterson, R.L. Benallie, A.M. Bradford, S.C. Pias, J. Yazzie, S.N. Lor, Z.M. Haulsee, C.K. Park, D.L. Johnson, L.R. Rohrschneider, A. Spuches, B.A. Lyons, Dimerization in the Grb7 protein, J. Mol. Recogn. 25 (8) (2012) 427–434.

[75] S.C. Pias, T.A. Peterson, D.L. Johnson, B.A. Lyons, The intertwining of structure and function: proposed helix-swapping of the SH2 domain of Grb7, A regulatory protein implicated in cancer progression and inflammation, Crit. Rev. Immunol. 30 (3) (2010) 299–304.

[76] L.Q. Dong, S. Porter, D. Hu, F. Liu, Inhibition of hGrb10 binding to the insulin receptor by functional domain-mediated oligomerization, J. Biol. Chem. 273 (28) (1998) 17720–17725.

[77] E.G. Stein, R. Ghirlando, S.R. Hubbard, Structural basis for dimerization of the Grb10 Src homology 2 domain. Implications for ligand specificity, J. Biol. Chem. 278 (15) (2003) 13257–13264.

[78] S. Nouaille, C. Blanquart, V. Zilberfarb, N. Boute, D. Perdereau, A.F. Burnol, T. Issad, Interaction between the insulin receptor and Grb14: a dynamic study in living cells using BRET, Biochem. Pharmacol. 72 (11) (2006) 1355–1366.

[79] I. García-Palmero, Functional Implication of the Calmodulin-Binding Domain of the Adaptor Protein Grb7, Doctoral Thesis, Universidad Autónoma de Madrid, 2012, pp. 1–215, https://repositorio.uam.es/handle/10486/129560.

[80] A. Villalobo, H. Ishida, H.J. Vogel, M.W. Berchtold, Calmodulin as a protein linker and a regulator of adaptor/scaffold proteins, Biochim. Biophys. Acta Mol. Cell Res. 1865 (3) (2018) 507–521.

[81] N. Hayashi, M. Matsubara, A. Takasaki, K. Titani, H. Taniguchi, An expression system of rat calmodulin using T7 phage promoter in Escherichia coli, Protein Expr. Purif. 12 (1) (1998) 25–28.

[82] S.R. Stateva, V. Salas, G. Benaim, M. Menéndez, D. Solís, A. Villalobo, Characterization of phospho-(tyrosine)-mimetic calmodulin mutants, PloS One 10 (2015), e0120798.

[83] A. Alaimo, C. Malo, P. Areso, K. Aloria, O. Millet, A. Villarroel, The use of dansyl-calmodulin to study interactions with channels and other proteins, Methods Mol. Biol. 998 (2013) 217–231.

[84] U.K. Laemmli, Cleavage of structural proteins during the assembly of the head of bacteriophage T4, Nature 227 (5259) (1970) 680–685.

[85] O. González-Fernández, A. Jiménez, A. Villalobo, Differential p38 mitogen-activated protein kinase-controlled hypophosphorylation of the retinoblastoma protein induced by nitric oxide in neuroblastoma cells, Free Radic. Biol. Med. 44 (3) (2008) 353–366.